engineering proceedings

Proceeding Paper

Dynamic Response of a Sono-Electrolyzer under PV Supply for Hydrogen Production: A Modelling Approach for the Kinetic and Energetic Assessment under Northern Algerian Meteorological Conditions †

Nour Hane Merabet [1,2,3,*] and Kaouther Kerboua [2]

1 Center of Applied Research, Karlsruhe University of Applied Sciences, Moltkestr. 30, 76133 Karlsruhe, Germany
2 Department of Process Engineering and Energetics, National Higher School of Technology and Engineering, Annaba 23005, Algeria; k.kerboua@esti-annaba.dz
3 Laboratory of Technologies of Energetic Systems E3360100, National Higher School of Technology and Engineering, Annaba 23005, Algeria
* Correspondence: merabet.nourhane@h-ka.de
† Presented at the 4th International Electronic Conference on Applied Sciences, 27 October–10 November 2023; Available online: https://asec2023.sciforum.net/.

Abstract: The experimental work is based on the PV solar powered membraneless KOH alkaline sono-electrolyzer using indirect continuous sonication under real meteorological conditions. The site of the study (36.9° N, 7.77° E) is located at the extreme North-East of Algeria, covering the semester ranging from March to September. A validated semi-empirical model for the dynamic assessment of the global incident solar radiation is adopted, in association with a fundamental model based on the electrical analogy of the electrolytic cell. The experimental setup and measurements coupled to the preliminary numerical model led to a fraction of electrode coverage of 37% with a maximum recovery of 13% and 10% in ohmic and cell voltages, respectively. The characterization of the sonication system through the calorimetric technique demonstrated an acoustic efficiency of 13.7%.

Keywords: green hydrogen; sono-electrolysis; cavitation; ohmic resistance; MatLab modeling

Citation: Merabet, N.H.; Kerboua, K. Dynamic Response of a Sono-Electrolyzer under PV Supply for Hydrogen Production: A Modelling Approach for the Kinetic and Energetic Assessment under Northern Algerian Meteorological Conditions. *Eng. Proc.* **2023**, *56*, 117. https://doi.org/10.3390/ASEC2023-15326

Academic Editor: Simeone Chianese

Published: 26 October 2023

1. Introduction

As an energy carrier with the advantages of high efficiency, cleanliness and sustainability, hydrogen has become a research hot topic [1]. Numerous studies have suggested that hydrogen produced from renewable energy sources, such as solar and wind, will have a major influence on global energy supplies in the near future. More specifically, the combination of solar photovoltaic energy with water electrolysis and battery is regarded as the most sustainable, suitable and clean pathway to H_2 production [2]. On an industrial scale, the most utilised and commercialised technologies for water electrolysis are alkaline electrolysis and proton exchange membrane which are based on the water splitting through the following reaction [3]:

$$H_2O \rightarrow H_2 + \frac{1}{2}O_2.$$

Solar electrolysis hydrogen production has been the subject of several studies, where very early, Bilgen [4] has attempted to develop a mathematical model for the determination and optimisation of the thermal and economic of performance of large-scale photovoltaic electrolyser systems. Sellami and Loudiyi [5] also investigated the effect of electrolyte's nature on the amount of produced hydrogen, while Dahbi et al. [6] investigated the possibility of the system's optimisation via MPPT implementation and the control of water flow injected. Burton et al. [7] reported the means of energy efficiency improvement using magnetic fields and high-voltage electric fields, light energy and ultrasonic fields. In our recent study [8], the effect of ultrasound on a Pv solar water electrolysis for hydrogen production was conducted experimentally and by means of modeling for a short period of one day under real meteorological conditions.

In the present study, a modeling study of hydrogen production via membraneless sono-electrolysis under indirect continuous sonication and real meteorological conditions was conducted: 25% KOH electrolyte and nickel plate electrodes were used, as well as MatLab modeling in order to assess the kinetic and the energy efficiency of hydrogen production based on the mathematical model of solar irradiation, PV panel and the alkaline electrolyzer.

2. Materials and Methods

A two-chamber electrolysis cell of 300 mL was used. Table 1 shows the parameters that were applied.

Table 1. Properties of the adopted system.

Site and Angles Parameters		PV Panel Parameters		Sono-Electrolysis Parameters	
Geographical coordinates	36.9° N, 7.77° E	Cell type	Monocrystalline	Electrolyte concentration	25% w/w, 4.46 M KOH
Albedo ρ	0.2	Short circuit current (Isc)	1.8 A	Sonication	Indirect continuous
Solar declination	$\delta = 23.45\ \sin(\frac{360}{365}(284 + N)$	Open circuit voltage (Voc)	21.52 V	Frequency and power	40 kHz and 60 W_e
Hour angle	$\omega = 15(TST - 12)$	Maximum power (Pmax)	30 W	Electrode material	Nickel plates

MatLab modeling

The adopted modeling part is based on the mathematical models of (i) solar irradiation, (ii) PV solar model, (iii) and water electrolysis.

Solar irradiation model

The global radiation on tilted surface G is calculated according to Equation (1) [9]:

$$G = D_\beta + B_\beta + R_g, \tag{1}$$

where D_β is the diffuse radiation, B_β and R_g are the beam and reflected radiation. In the adopted model, diffused radiation D_β is estimated according to the anisotropic model of Hay [9] as in Equation (2):

$$D_\beta = D_d(f_{Hay}\left(\frac{\cos\theta}{\cos\theta_z}\right) + \left(\frac{1+\cos\beta}{2}\right)(1 - f_{Hay}), \tag{2}$$

$$f_{Hay} = \frac{D_b}{E_{xt}}, \tag{3}$$

where R_g is the reflected radiation which is the fraction of global radiation that is reflected by the Earth's surface and any other obstructing object and is calculated according to Equation (4):

$$R_g = H\rho\left(\frac{1-\cos\beta}{2}\right). \tag{4}$$

The direct beam irradiance on a tilted surface can be calculated using Equation (5):

$$D_\beta = r_\beta D_b, \tag{5}$$

where r_β represents the ratio of the hourly radiation received by an inclined surface to that received by a horizontal surface outside the Earth's atmosphere and is calculated using the following equation [9]:

$$r_\beta = \frac{E_{0\beta}}{E_{xt}} \approx \frac{\cos\theta}{\cos\theta_z}. \tag{6}$$

In the previous equations, E_{xt}, θ and θ_z are the extraterrestrial radiation, the incidence angle and the zenith angle that are calculated according to specific equations [9].

PV panel model

The current delivered from the PV panel is represented as given in Equation (7) [10]:

$$I = I_{pv} - I_d - I_{sh}. \tag{7}$$

In the expression of I, I_{pv}, I_d and I_{sh} are the light current, diode current and shunt current, respectively, and they can be expressed as follows [11,12]:

$$I_{pv} = \frac{(I_{pv0} + K\Delta T)G}{G0}, \tag{8}$$

$$I_d = I_0\left(\exp\left(\frac{R_s I + V}{V_t a}\right) - 1\right), \tag{9}$$

$$I_{sh} = \frac{V + R_s I}{R_p}. \tag{10}$$

Water electrolysis system

Electrolyser's voltage U_{cell} is dependent on the current produced from the PV panel, potential involved E_{rev} is the reversible voltage, U_{act} is activation voltage, U_{Ohm} is ohmic voltage and U_{Conc} is concentration voltage, which are expressed according to equations below [13–15]:

$$U_{cell} = E_{rev} + U_{act} + U_{Ohm} + U_{Conc}, \tag{11}$$

$$E_{rev}(T, P) = E_{rev}(T) + \frac{RT}{ZF}\ln\left(\frac{P_v{}^*(P - P_v)^{1.5}}{P_v}\right), \tag{12}$$

$$U_{act} = \frac{2.3026\ RT}{ZFa_a}\log\left(\frac{I_a}{I_{0a}}\right) + \frac{2.3026\ RT}{ZFa_c}\log\left(\frac{I_c}{I_{0c}}\right), \tag{13}$$

$$U_{ohm} = I\left(R_{cell} + R_{electrodes} + R_{electrolyte} + R_{electrical}\right), \tag{14}$$

$$U_{conc} = \frac{RT}{ZF}\left(\ln\left(1 - \left(\frac{I}{I_{lim}}\right)\right)\right). \tag{15}$$

Calorimetric characterization of sono-electrolysis

As the propagation of the ultrasound waves within the electrolyte increases the electrolyte's temperature, an evaluation of the acoustic power transferred to the electrochemical cell was conducted. There, the power of the ultrasound transmitted to the electrolyte is calculated by means of equation below [16]:

$$P_s = \frac{m_{KOH} C_p dT}{dt}, \tag{16}$$

where m_{KOH} is the mass of the alkaline electrolyte, C_p and dT are the heat capacity of the electrolyte at constant pressure and temperature change within the monitoring time.

Kinetics of hydrogen production

According to Faraday's law [17], the rate of hydrogen gas produced by water electrolysis is equal to the electrical charge consumed by the cell which is expressed according to Equation (17):

$$\dot{m}_{H_2} = \frac{NIM_{H_2}}{ZF}\eta_F, \tag{17}$$

where $\dot{m}_{H_2}$ is the mass flow of hydrogen production by the electrolyzer in g/s, M_{H_2} and N are the cell number of electrolyser and molar mass, respectively, and η_F represents the Faraday efficiency.

3. Results and Discussion

3.1. Kinetics of Hydrogen Production

Figure 1a shows the simulated hourly solar irradiance and delivered current f for each month. It is clear that the solar irradiation and the delivered current are at their highest values during the summer period. The highest values of solar irradiation, 992 W/m^2, are reached in the summer period during the month of May around solar noon, while the maximum delivered current of 1.6 A is recorded during the month of June.

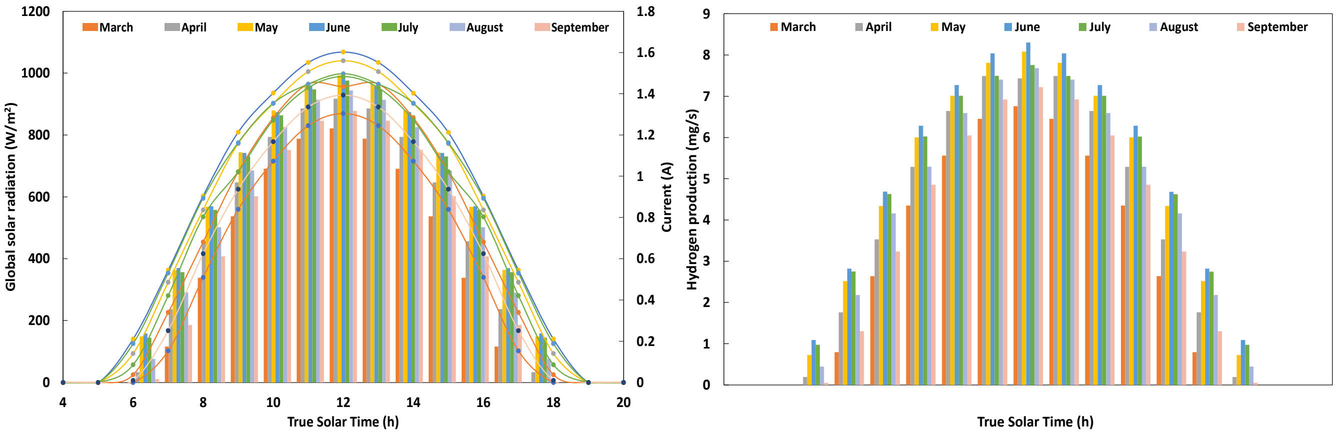

(**a**) (**b**)

Figure 1. Simulated results of monthly (**a**) hourly solar irradiation and delivered current; (**b**) kinetics of hydrogen production and delivered current.

The kinetics of hydrogen production according to the hourly delivered current are shown in Figure 1b. The kinetics of hydrogen production increase with increasing current according to Faraday's law and reaches its maximum of 8 µmol/s in June around solar noon.

3.2. Sono-Electrolysis Results

According to the obtained results and based on a calorimetric study [16], the characterisation of the sonication system demonstrated an acoustic efficiency of 13.7% when considering the delivered power of 60 W. This means that the remainder of the power consumed is dissipated as heat to the electrolyte and the surrounding environment.

Figure 2a,b shows the average cell resistance and cell voltage as a function of the coverage of the electrode with air bubbles. The electrode bubble coverage in the presence and absence of ultrasound is 37% and 82%, respectively, based on the previous experimental results [8]. Thus, it can be seen that in the quiescent system, the ohmic voltage and cell voltage range from 2.6 to 3.5 V and from 4.1 to 4.8 V, respectively, depending on the month, whereas under sonication they decrease to 2.25 to 2.8 V for the ohmic voltage and to 3.7 to 4.3 V for the cell voltage.

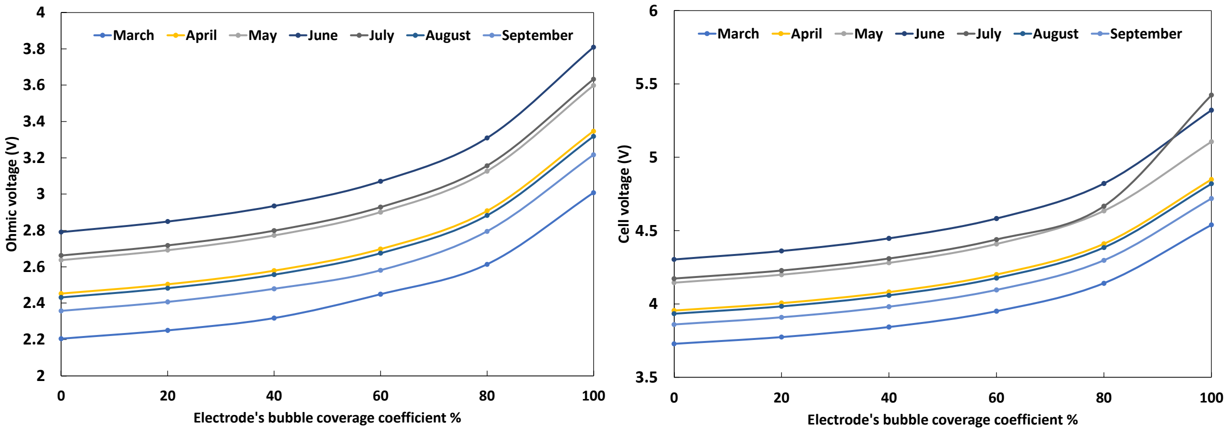

(**a**) (**b**)

Figure 2. Simulated results of monthly average (**a**) ohmic voltage; (**b**) cell voltage in function of electrode's bubble coverage.

As it is assumed in the literature, the bubble presence in the electrolyte and on the electrode surface increases the ohmic resistance and voltage and thus the power consumption. It was observed that the higher the current supplied by the solar panel, the higher the hydrogen production kinetics and the higher the bubble and ohmic resistance. The integration of the sonication reduces the ohmic voltage by about 13.5–20% and the cell voltage by 9.7–10.4%, depending on the month. This means that for the same feed current, the hydrogen kinetics described by the mass flow rate are more important due to the effective desorption effect of sonication.

4. Conclusions

In the present study, hydrogen production via sono-electrolysis powered by a PV solar system was performed using a detailed modeling pathway. The study covered the period of time from March to September under real meteorological conditions during the whole representative days. It was revealed that only 13.7% of the consumed power of the sonicator was transferred to the electrochemical cell. In addition, the highest hydrogen production was recorded during summer, when irradiation reached its maximum. In addition, under sonication conditions, a maximum recovery of 13% and 10% in ohmic and cell voltages, respectively, was recorded.

Author Contributions: N.H.M.: Modeling; Simulation, 1st draft; Review of the final version. K.K.: Projet supervision; Review of the final version; Validation. All authors have read and agreed to the published version of the manuscript.

Funding: This research was funded by German academic exchange service DAAD, within the framework of the exchange program 57588368 Research Grants—Binationally Supervised Doctoral Degrees/Cotutelle, 2022/23.

Institutional Review Board Statement: Not applicable.

Informed Consent Statement: Not applicable.

Data Availability Statement: Data are contained within the article.

Conflicts of Interest: The authors declare no conflict of interest.

References

1. Zhang, J.; Ling, B.; He, Y.; Zhu, Y.; Wang, Z. Life cycle assessment of three types of hydrogen production methods using solar energy. *Int. J. Hydrogen Energy* **2022**, *47*, 14158–14168. [CrossRef]
2. Gutiérrez-Martín, F.; Amodio, L.; Pagano, M. Hydrogen production by water electrolysis and off-grid solar PV. *Int. J. Hydrogen Energy* **2021**, *46*, 29038–29048. [CrossRef]

3. Nou, H.M.; Kaouther Kerboua, O.H. Converting PV solar energy to green hydrogen. In *Reference Module in Earth Systems and Environmental Sciences*; Elsevier: Amsterdam, The Netherlands, 2023; pp. 1–10.
4. Bilgen, E. Solar hydrogen from photovoltaic-electrolyzer systems. *Energy Convers. Manag.* **2001**, *42*, 1047–1057. [CrossRef]
5. Sellami, M.H.; Loudiyi, K. Electrolytes behavior during hydrogen production by solar energy. *Renew Sustain. Energy Rev.* **2017**, *70*, 1331–1335. [CrossRef]
6. Dahbi, S.; Aboutni, R.; Aziz, A.; Benazzi, N.; Elhafyani, M.; Kassmi, K. Optimised hydrogen production by a photovoltaic-electrolysis system DC/DC converter and water flow controller. *Int. J. Hydrogen Energy* **2016**, *41*, 20858–20866. [CrossRef]
7. Burton, N.A.; Padilla, R.V.; Rose, A.; Habibullah, H. Increasing the efficiency of hydrogen production from solar powered water electrolysis. *Renew. Sustain. Energy Rev.* **2021**, *135*, 110255. [CrossRef]
8. Hane, N.; Merabet, K.K. Green hydrogen from sono-electrolysis: A coupled numerical and experimental study of the ultrasound assisted membraneless electrolysis of water supplied by PV. *Fuel* **2024**, *356*, 129625.
9. Maleki, S.A.M.; Hizam, H.; Gomes, C. Estimation of hourly, daily and monthly global solar radiation on inclined surfaces: Models re-visited. *Energies* **2017**, *10*, 134. [CrossRef]
10. Ghribi, D.; Khelifa, A.; Diaf, S.; Belhamel, M. Study of hydrogen production system by using PV solar energy and PEM electrolyser in Algeria. *Hydrog. Energy* **2013**, *38*, 8480–8490. [CrossRef]
11. Villalva, M.G.; Gazoli, J.R.; Filho, E.R. Comprehensive Approach to Modeling and Simulation of Photovoltaic Arrays. *IEEE Trans. Power Electron.* **2009**, *24*, 1198–1208. [CrossRef]
12. Rahim, A.H.A.; Salami, A.; Fadhlullah, M.; Hanapi, S.; Sainan, K. Optimization of direct coupling solar PV panel and advanced alkaline electrolyzer system. *Energy Procedia* **2015**, *79*, 204–211. [CrossRef]
13. LeRoy, R.L.; Bowen, C.T.; LeRoy, D.J. The Thermodynamics of Aqueous Water Electrolysis. *J. Electrochem. Soc.* **1980**, *127*, 1954–1962. [CrossRef]
14. Azad, A.K.; Khan, M.M.K. *Bioenergy Resources and Technologies*; Academic Press: Cambridge, MA, USA, 2021.
15. Allen, J.B.; Larry, R.; Faulkner, H.S.W. *Elechtrochemical Methods, Fundamentals and Applications*; Wiley: Hoboken, NJ, USA, 2022.
16. Kerboua, K.; Merabet, N.H. Sono-electrolysis performance based on indirect continuous sonication and membraneless alkaline electrolysis: Experiment, modelling and analysis. *Ultrason. Sonochem.* **2023**, *96*, 106429. [CrossRef] [PubMed]
17. Sanchez, M.; Amores, E.; Rodrıguez, L.; Clemente-Jul, C. Semi-empirical model and experimental validation for the performance evaluation of a 15 kW alkaline water electrolyzer. *Int. J. Hydrogen Energy* **2018**, *43*, 1–14. [CrossRef]